CONF-890403--20

DE89 012342

Numerical Methods for Stellarator Optimization*

R. N. Morris, C. L. Hedrick, S. P. Hirshman,
J. F. Lyon, J. A. Rome

Oak Ridge National Laboratory
Oak Ridge, Tennessee 37831

ABSTRACT

A numerical optimization procedure utilizing an inverse 3-D equilibrium solver, a Mercier stability assessment, a deeply-trapped-particle loss assessment, and a nonlinear optimization package has been used to produce low aspect ratio ($A = 4$) stellarator designs. These designs combine good stability and improved transport with a compact configuration.

The development of 3-D plasma analysis tools for the optimization of stellarator designs is important for the current ATF-II studies and beyond. The subject of this work, low aspect ratio studies, presents the challenge of reconciling MHD stability with favorable neoclassical transport in a single compact device. Toroidal effects, which are enhanced at low aspect ratios, often tend to influence MHD and transport properties in opposing ways and this work will present a numerical procedure that seeks an optimal balance between the two. The parameter space over which the optimization is carried out is defined by a set of Fourier harmonic coefficients describing the boundary of the plasma. The basis of the nonlinear optimal search scheme is formed by varying the boundary around a tentative design and assessing the changes in Mercier stability and the transport of deeply trapped particles in the altered configuration. The success of this procedure depends on the proper evaluation of the plasma parameters as well as the existence of an adequate initial configuration. The rapid computations of inverse equilibria, stability, and confinement criteria are also crucial. Plasma parameters of interest include iota profile, magnetic well profile, MHD stability, particle transport, and configuration complexity.

Because of the complexity and time-consuming nature of most plasma physics calculations, the MHD stability and transport evaluations have to be limited in scope. The Mercier criterion [1] has been chosen for the MHD stability calculation and the "B minimum" ($B_{\min}$) contours [2] have been selected for calculation of the transport criterion. In both cases the figure of merit used for the optimization is a percentage of the appropriate maximum as measured in normalized flux space, ψ.

*Research sponsored by the Office of Fusion Energy, under contract DE-AC05-84OR21400 with Martin Marietta Energy Systems, Inc.

The Mercier stability module returns the percentage of the plasma that is unstable to high order localized ideal MHD modes outside of the central ($0.1 < \psi$) plasma region. The transport module concentrates only on deeply trapped particles and returns the width, in flux space, of the last closed $B_{\min}$ contour. Also available is an option to determine the offset of the $B_{\min}$ contours from the magnetic axis.

It is useful for the boundary Fourier expansions of the three-dimensional inverse MHD equilibria to have a unique poloidal angle, in order to prevent the problems of an ill defined convergence path in Fourier space. To this end we have chosen to use the following form to represent the boundary [3]:

$$R = \sum_{n=0}^{N} R_{\mathrm{on}} \cos n\phi + \sum_{n=-N}^{N} R_{1n} \cos(\theta - n\phi) + \bar{r} \cos\theta$$

$$Z = \sum_{n=0}^{N} Z_{\mathrm{on}} \sin n\phi - \sum_{n=-N}^{N} R_{1n} \sin(\theta - n\phi) + \bar{r} \sin\theta$$

$$\bar{r} = \sum_{n=0}^{N} r_{\mathrm{on}} \cos n\phi + \sum_{m=3,n}^{N} r_{\mathrm{mn}} \cos(m\theta - n\phi)$$

where ϕ is the toroidal angle and θ is the poloidal angle. Seven of these coefficients are allowed to vary during the course of the optimization. They are: R_{0N_p}, Z_{0N_p}, R_{10}, R_{1N_p}, r_{30}, r_{0N_p}, and r_{3N_p}, with $r_{00} = 1 - R_{10}$ to keep the aspect ratio fixed during the iterations. The remainder of the harmonics, 20-30 total, are zero at the boundary and are chosen to provide numerical accuracy. The number of field periods, N_p, also remains fixed during the course of the optimization. Finally, the varying coefficients are scaled to order 1 before being used in the numerical process to insure numerical stability.

The optimization process is implemented by forming a loop composed of a multi-dimensional nonlinear optimization routine (MNOR), a three dimensional inverse plasma equilibrium solver [4], a routine for assessing Mercier stability [5], an analysis of plasma transport, and finally, a function that combines this information into a single numerical value for use by the MNOR. A typical iteration proceeds by the MNOR package providing the plasma equilibrium solver with the Fourier coefficients of a trial boundary. The equilibrium solver then computes the plasma profiles of iota, flux, magnetic well, etc. for use by the Mercier and transport modules. These modules return figures of merit and the computed criteria are combined in a function of the form,

$$F = x_a TANH(\gamma x_a) + x_e TANH(\gamma x_e) + \alpha L_M - \delta L_B;$$
$$x_a = (\iota_a - \iota_{ao})/\iota_{ao},\ x_e = (\iota_e - \iota_{eo})/\iota_{eo}$$

where ι_a and ι_e are the computed rotational transform at the magnetic axis and plasma edge, respectively, and ι_{ao} and ι_{eo} are the corresponding desired transform values; L_M is the percentage of the plasma that is Mercier unstable, L_B is the percentage width of the last closed $B_{\min}$ contour, and α, γ, δ are constants chosen

to steer the optimization in the desired direction. The $TANH$ function prevents the optimization function from increasing too rapidly when the iota values differ greatly while providing a sum-of-squares behavior near the optimum. Experience has shown that this form provides the most reliable results. The constants δ and α fall in the ranges, $1 < \delta < 10$ and $3 < \alpha < 30$ with $\gamma \sim 10.0$. Unfortunately these values can only be determined empirically and require many computer runs to estimate the best values.

The MNOR is a quasi-newton method using finite differences; it is the E04JBF subroutine contained in the NAG library [6,7]. Since subroutines of this nature can find only local minima, the path from large aspect ratio devices to small ones is best located by an incremental process. In this work an approximate representation of the current ATF device was used as the starting point and the aspect ratio and number of field periods were reduced by small steps until the goal of $A = 4$ was reached. At each converged step small perturbations were made in the boundary to examine the local parameter space. This process does not require that all the optimization modules be used; one may wish to focus on only a couple of the criteria to conserve effort until the desired aspect ratio/field period region is reached.

The results of this process at $\langle\beta\rangle = 0$ are shown in Table I. In these cases the optimization included only $\iota_a(\iota_{ao} = 0.35)$, $\iota_e(\iota_{eo} = 1.0)$, L_B and the magnetic well; rather than employ the complete Mercier criterion, the entries in Table I were only required to have a magnetic well with a finite width. Note that by keeping the ratio of field periods to aspect ratio in the range of 1.5-1.6 the iota and L_B values are preserved as the aspect ratio is reduced.

The aspect ratio is defined as $A = \pi R_a \sqrt{2R_a/V}$, where V is the plasma volume and R_a is the radius of the plasma center which is approximately the edge value of the R_{00} harmonic. For the cases shown in Table I, the aspect ratio may be very closely approximated as the edge value of the R_{00} harmonic because of the selected normalization. This value is shown in parentheses in Table I.

The last case in Table I was obtained by examining the parameters locally around the previous 6 field period case. Note that a large improvement in L_B came at the expense of the well depth. This compromise also appears in calculations that use the Mercier stability criterion instead of finite well width and underlines the conflict between stability and transport.

Currently the optimization can be performed only at a fixed plasma pressure. Fortunately, our calculations show that if the plasma is stable at a given average beta, $\langle\beta\rangle$, it will also be stable at lower $\langle\beta\rangle$ with the same pressure profile. Selection of the plasma pressure profile is somewhat difficult, but a modestly peaked profile with weak edge gradients appears to give the most useful results. The present work uses a pressure profile of the form

$$p(\psi) = p_0(1-\psi)^2(1-\psi^2)$$

where ψ is the normalized toroidal flux and p_0 can be adjusted to provide the necessary $\langle\beta\rangle$.

The results of an optimization on a $N_p = 6$, $A = 4$ device at $\langle\beta\rangle = 5\%$ is shown in Figs. 1 and 2. The $\langle\beta\rangle = 0$ fixed boundary result, obtained by using the optimized $\langle\beta\rangle = 5\%$ boundary with $p_0 \sim 0$, is shown in Fig. 1. Starting at the

top left and moving clockwise, one has the flux surfaces at $\phi = 0$, the iota profile vs ψ, the magnetic well vs ψ, and the $B_{\min}$ contours ($L_B = 0.9$). The $\langle\beta\rangle = 5\%$ case is shown in Fig. 2. Starting at the top left and moving clockwise, one has the flux surfaces at $\phi = 0$ (note the shift), the iota profile vs ψ, the Mercier criterion vs ψ, and the $B_{\min}$ contours ($L_B = 0.8$). The minimum in the Mercier value takes place at the $\iota = 1/3$ surface. The $B_{\min}$ contours become increasingly shifted as $\langle\beta\rangle$ increases, a factor that adversely affects transport.

We conclude that promising low aspect ratio stellarator designs may exist and that the described numerical process is a useful tool for locating them. Further work remains to be done to examine the parameter space and numerical sensitivity issues.

REFERENCES

[1] BAUER, F., BETANCOURT, O., GARABEDIAN, P. A., "Magnetohydrodynamic Equilibrium and Stability of Stellarators," Springer-Verlag, New York (1984).

[2] HEDRICK, C. L., CARY, J. R., TOLLIVER, J. S., "Adiabatic and Full Guiding Center Motion in 3-D Toroidal Systems," to be published.

[3] HIRSHMAN, S. P., WEITZNER, H., Phys. Fluids **28**, 1207 (1985).

[4] HIRSHMAN, S. P., WHITSON, J. C., Phys. Fluids **26**, 3553 (1983).

[5] DOMINGUEZ, N., private communication.

[6] Numerical Algorithms Group, Inc., Downers Grove, Illinois 60515-1263.

[7] GILL, P. E., MURRAY, W., Journal of the Institute of Mathematics and Its Applications, **9** 91 (1972).

TABLE I

Aspect Ratio	Field Period	ι Axis	ι Edge	L_B	Magnetic Well
7.8 (8)	12	0.42	1.0	0.61	2%
5.13 (5.33)	8	0.36	0.95	0.59	2.3%
3.9 (4.0)	6	0.36	0.94	0.58	3.2%
3.3 (3.33)	5	0.35	0.92	0.57	3.5%
3.9 (4.0)	6	0.33	0.98	0.87	1.9%

FLUX SURFACES

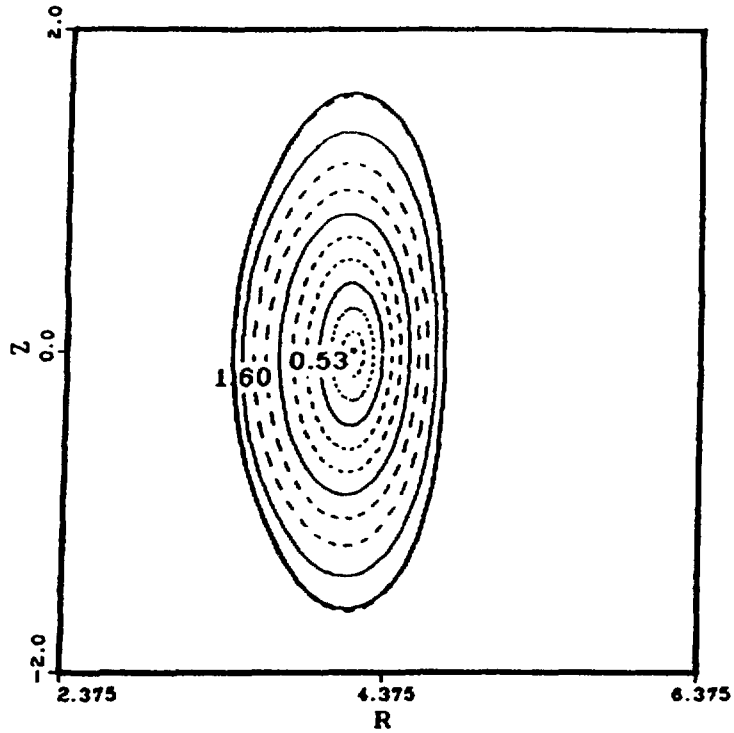

IOTA

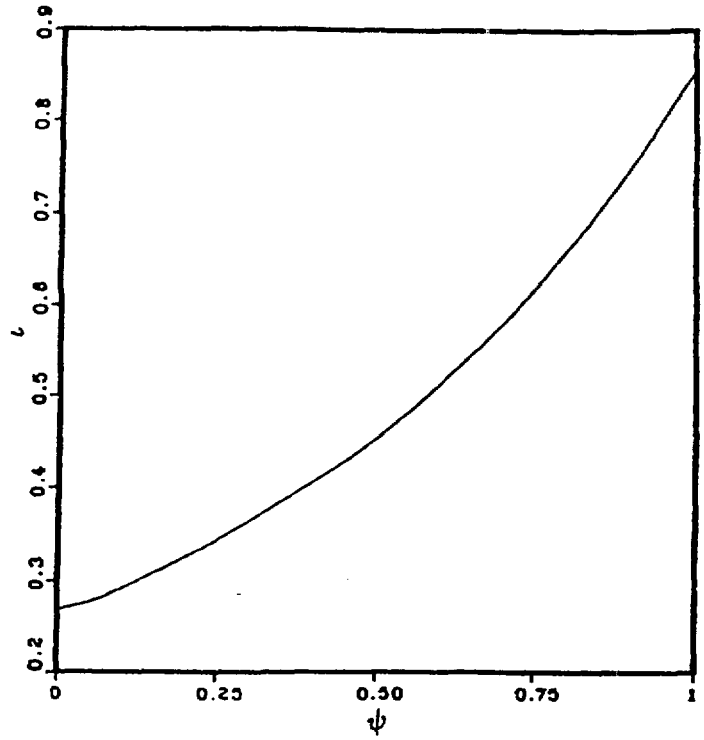

B_{min}

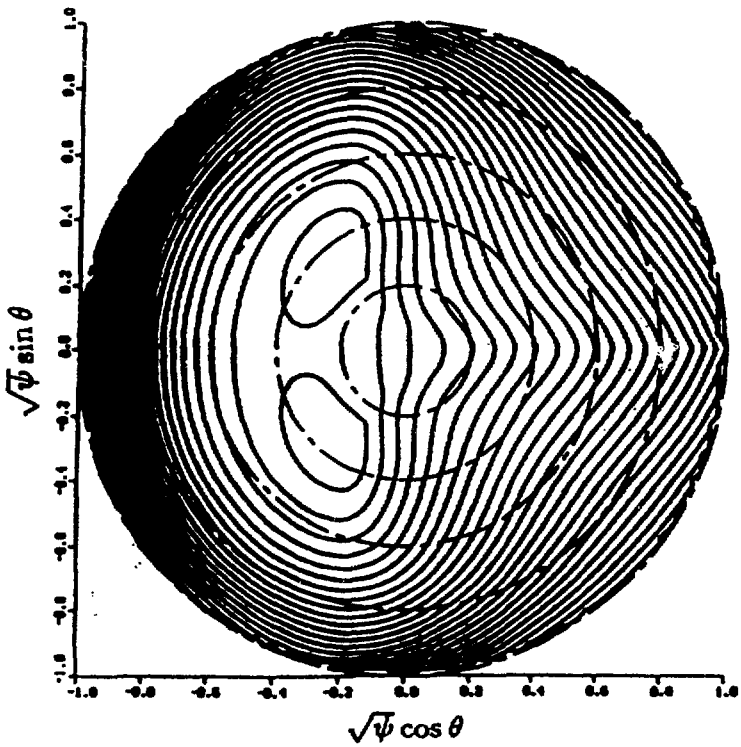

MAGNETIC WELL

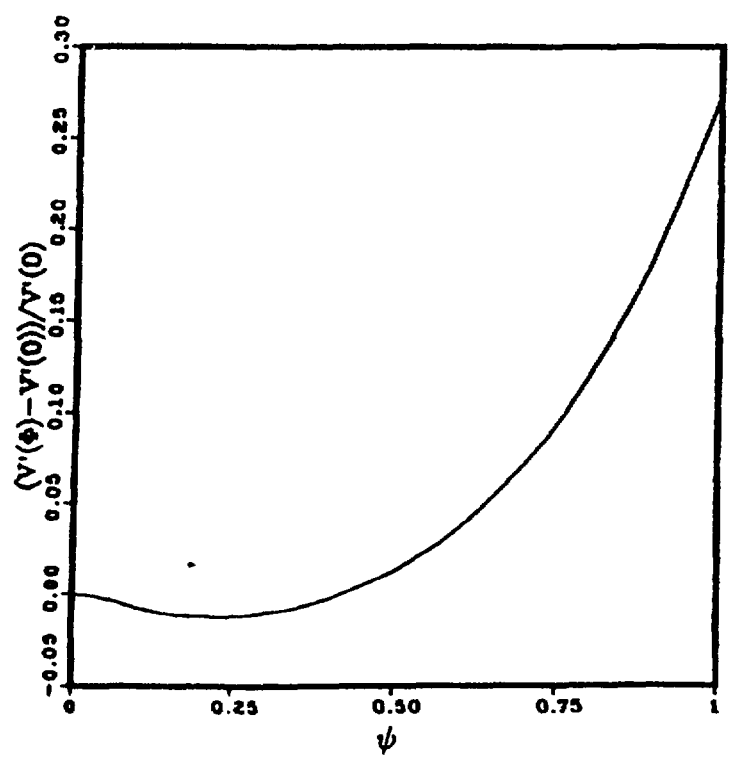

Figure 1

FLUX SURFACES

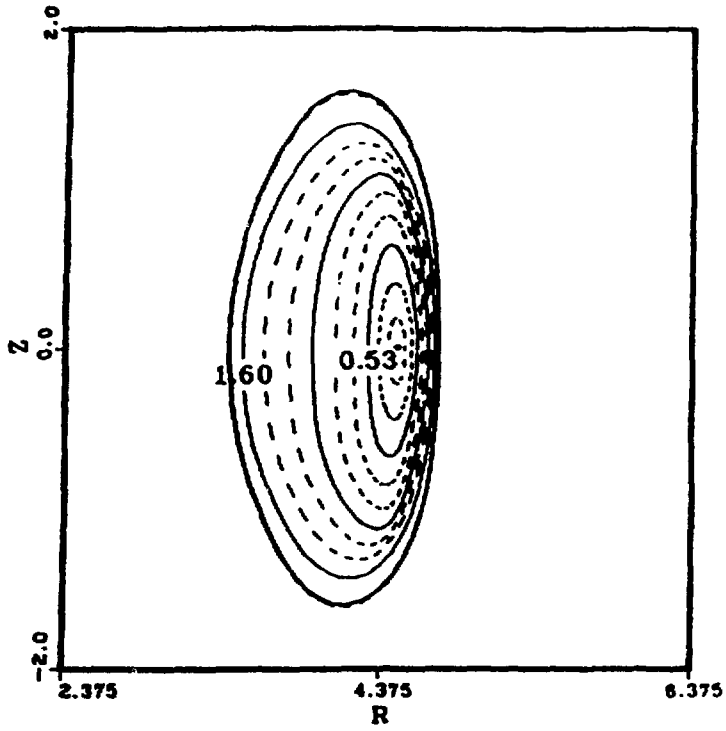

IOTA

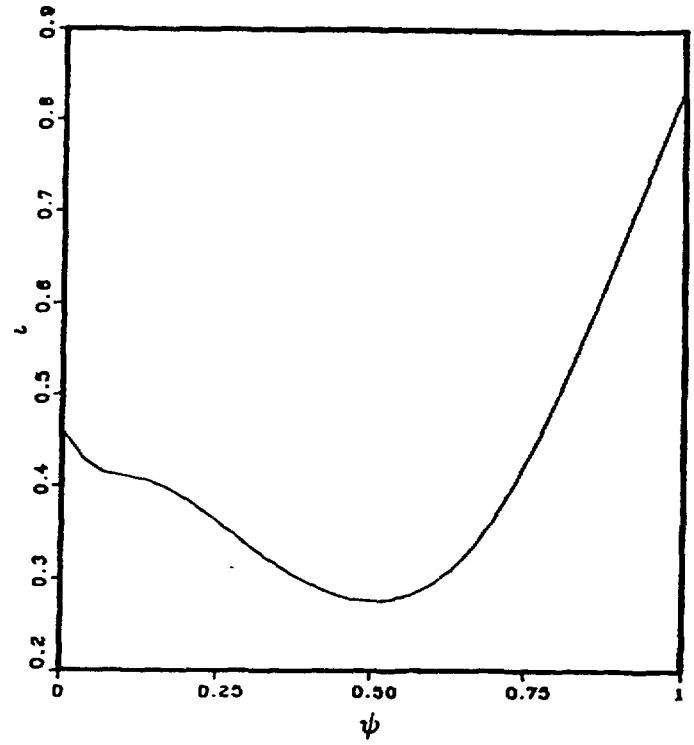

$B_{\min}$

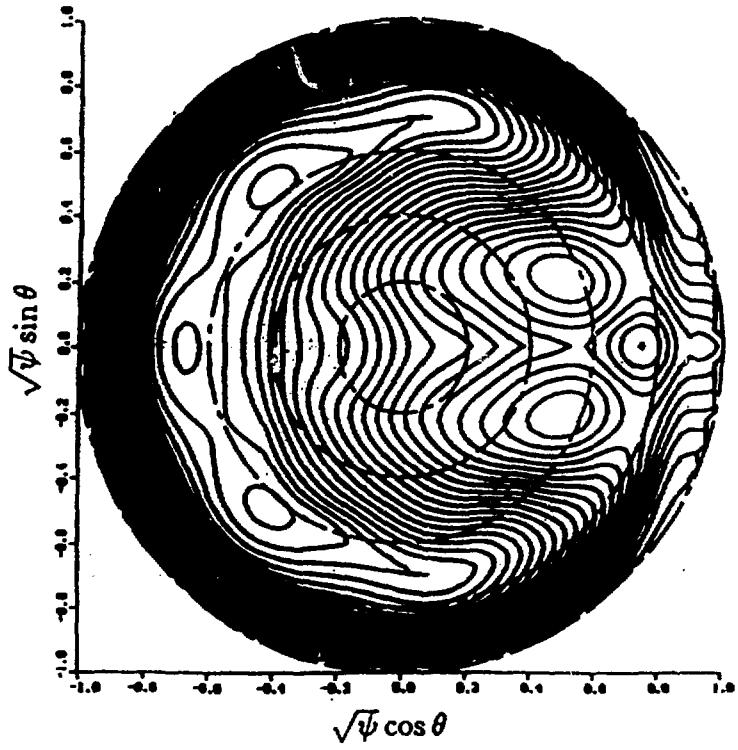

D_M

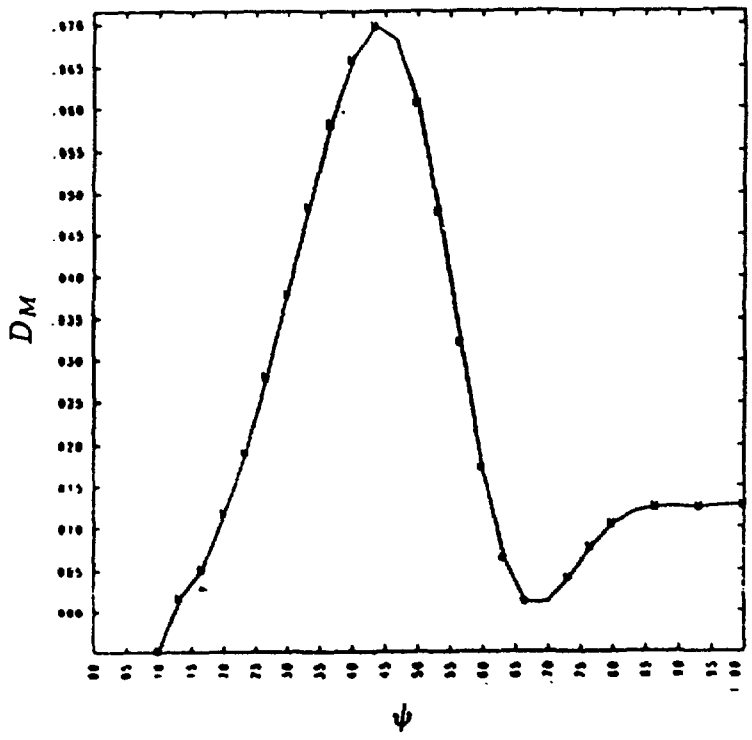

Figure 2

DISCLAIMER